Int J Ind Chem (2015) 6:329–338
DOI 10.1007/s40090-015-0055-7

RESEARCH

Afzelia quanzensis bark extract for green synthesis of silver nanoparticles and study of their antibacterial activity

Mambo Moyo[1] · **Makore Gomba**[1] · **Tichaona Nharingo**[1]

Received: 14 September 2014 / Accepted: 10 September 2015 / Published online: 24 September 2015

Abstract In the present study, *Afzelia quanzensis* bark extract was tested for the biosynthesis of silver nanoparticles (AgNPs). Based on UV–Vis spectrum analysis, the characteristic absorption band was observed at 427 nm. Furthermore, the size and shape of the nanoparticles ranged from 10 to 80 nm and were spherical in shape as observed through SEM analysis. In addition, the X-ray diffraction analysis showed that the silver nanoparticles are crystalline in nature and have a face-centred cubic structure. Based on FTIR analysis, the presence of phytochemical functional groups such as carboxyl (–C=O) and amine (N–H) in *Afzelia quanzensis* bark extract further confirmed the responsible reducing agents for nanoparticles formation. Interestingly, the synthesized silver nanoparticles at 50 mg/L concentration showed significant antibacterial activity against *Escherichia coli* and *Staphylococcus aureus*.

Keywords Biological synthesis · Silver nanoparticles · Bark extract · Antibacterial activity

Introduction

At present, nanotechnology is a rapidly developing field of importance since it deals with the synthesis and stabilization of different metal nanoparticles. Among the particles, silver nanoparticles (AgNPs) have become the focus of intensive research due to several important applications such as their use in bio-labelling, sensors, drug delivery system, antimicrobial agents and filters [1, 2]. The synthesized silver nanoparticles exhibit new or improved properties depending upon their size, morphology and distribution [3]. The production of pure and well-defined metal-based nanoparticles by chemical reduction [4], thermal treatment, irradiation [5] and laser ablation [6] have been reported. On one hand, organic solvents, toxic reducing agents, high-pressure and high-temperature conversion which are potentially dangerous to the environment are used [7]. Hence, a pressing need to shift from physical and chemical synthesis to 'green' chemistry and bioprocesses is of major interest.

In the last decade, the biosynthesis of nanoparticles has received increasing attention due to the growing need to develop environmentally benign technologies in material synthesis [8, 9]. Biological routes for the synthesis of metal nanoparticles by exploiting bacteria [10, 11], marine fungus *Penicillium fellutanum* [1], fungus *Aspergillus foetidus* [12], yeast [13, 14], enzymes [15] have been reported. However, one of the major drawbacks in using microbes for nanoparticle synthesis is the elaborate process of maintaining microbial cultures. The use of plant extracts for the synthesis of nanoparticles have gained momentum in recent years and could be advantageous over other environmentally benign biological processes by eliminating the elaborate process of maintaining cell cultures, being simply, eco-friendly and this could be an exciting possibility that is relatively unexplored and under exploited [16]. Green silver nanoparticles synthesis using various natural products like *Magnolia kobus* [17], *Acacia leucophloea* extract [18], *Zizyphus xylopyrus* bark extract [19], *aloevera* plant extract [20, 21], *Cinnamon zeylanicum* bark extract [22], *Curcuma longa* tuber powder [23] and *Jatropha curcas* [9] have been reported. However, the

✉ Mambo Moyo
moyom@msu.ac.zw

[1] Department of Chemical Technology, Faculty of Science, Midlands State University, P. Bag 9055, Senga, Gweru, Zimbabwe

potential of other plants as sources of biomaterial for the synthesis of new nanoparticles are yet to be entirely explored.

It has been reported that plants contain different phytochemical products [24] which are able to breakdown the silver nitrate, a complex hazardous chemical into Ag^+ and NO_3^- ions. In the process, the toxic Ag^+ ions are further reduced to the nontoxic (Ag^0) metallic nanoparticles through the use of different functional groups on the surface of the extract [25]. In the present study, we selected *Afzelia quanzensis*, Pod mahogany (English), Mujarakamba (Shona name in Zimbabwe) bark as a biomaterial for supplying the different phytochemicals required for the synthesis of silver nanoparticles and the mechanism involved in the synthesis is illustrated in Fig. 1. The plant is economic and abundantly available in Zimbabwe. It is a medium-sized to large deciduous tree and has a bark which is greyish-brown, flaking and leaving pale patches [26]. It produces fruits which consist of a large flattened pod, thickly woody, 10–17 cm, and splitting to reveal large, shiny black seeds with a bright red aril. In medicine, roots are used to treat gonorrhoea, chest pains, kidney problems, bilharzia, eye problems and snakebites, and a small piece of bark is applied to an aching tooth. The plant can be categorized as:

Taxonomy
Kingdom: Plantae
Division: Tracheophyta
Subdivision: Spermatophytina
Class: Magnoliopsida
Order: Fabales
Family: Fabaceae
Genus: *Afzelia* Sm.—mahogany
Species: *Afzelia quanzensis* Welw.—pod mahogany

In the present study, we used plant bark extracts for synthesis of silver nanoparticles by monitoring their conversion using UV–visible spectroscopy. We also investigated the effects of reaction conditions such as temperature, pH, quantities of bark extract and $AgNO_3$ concentration on the synthesis rate. The silver nanoparticles were further characterized by X-ray diffraction (XRD), scanning electron microscopy (SEM), energy dispersive X-ray (EDX) spectrometer, and Fourier transform infrared spectroscopy (FTIR). Furthermore, the antibacterial activity of the silver nanoparticles on a strain of *Escherichia coli* and *Staphylococcus aureus* was qualitatively evaluated by the zone inhibition method.

Materials and methods

Preparation of *Afzelia quanzensis* bark powder and extract

The bark was obtained from *Afzelia quanzensis* tree in Chivi rural district area, Zimbabwe. The bark was washed to remove any impurities and dried under sunlight for a week to completely remove the moisture. The bark was cut into small pieces, powdered in a mixer and then sieved using a 20-mesh sieve to get uniform size range. The sieved powder was used for all further studies. For the production of an extract, 50 g of powdered bark was added to a 500-mL Erlenmeyer flask containing 200 mL deionized water and then boiled for 15 min. After cooling, the mixture was filtered through Whatman filter paper no. 1 and the extract was kept at 4 °C prior to silver nanoparticles synthesis.

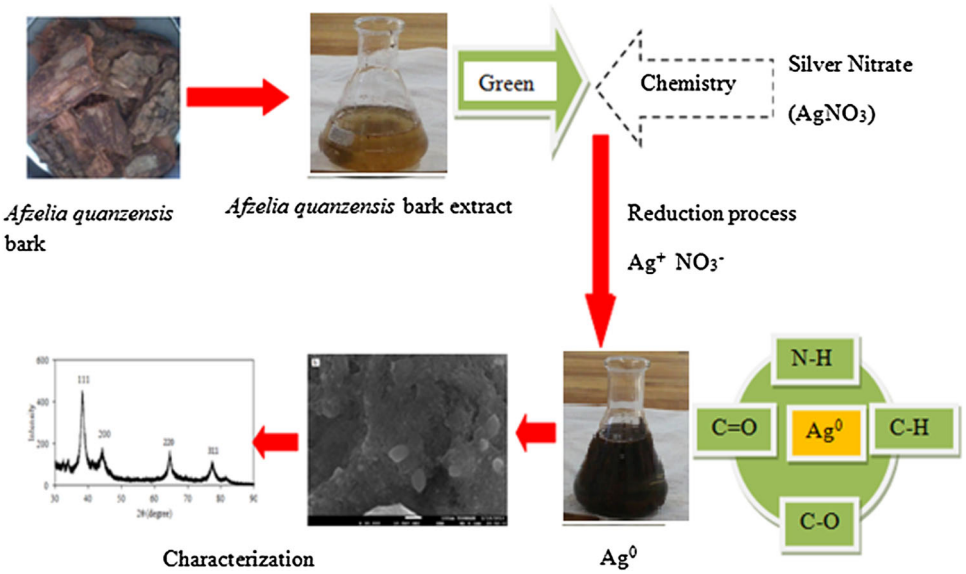

Fig. 1 Mechanism involved in the synthesis of silver nanoparticles using *Afzelia quanzensis* extract

Synthesis of silver nanoparticles

Silver nitrate ($AgNO_3$) analytical grade used as a precursor was purchased from Sigma-Aldrich (Pretoria, South Africa). For the AgNPs synthesis, 5 mL bark extract were added to 50 mL of 1 mM aqueous $AgNO_3$ solution in a 250-mL Erlenmeyer flask. The flask was then incubated in a rotary shaker at 160 rpm in the dark. The reduction of silver ions was routinely monitored visually for colour change at regular intervals. Thereafter, the silver nanoparticle solution thus obtained was purified by repeated centrifugation at 500 rpm for 20 min followed by re-dispersion of the pellet of silver nanoparticles into a 10 mL of deionized water. After freeze drying, lyophilization process was performed on the purified silver nanoparticles to obtain the powdered form which was stored in brown bottles prior to physical characterization and antibacterial activity.

Characterization

UV–Vis spectrophotometer analysis

The preliminary reduction of synthesized silver nanoparticles was monitored using UV–visible spectrophotometer (Shimadzu UV-1601, Japan) by scanning the absorbance spectra in the range of 300–600 nm. All sample solutions were diluted using a ratio of 1:10.

Electron microscopic study

SEM analysis of the synthesized silver nanoparticles was done using a Hitachi S-4500 SEM machine (Japan). A thin layer of gold was used to coat the samples through vacuum evaporation so that the nanoparticles conducts evenly and provides a homogeneous surface for analysis and imaging on an aluminium slab. The elemental analysis was performed using EDX (JEOL-JSM-5800LV, Tokyo, Japan) which is an attachment to the SEM. The sample powder of AgNPs was compressed to form tablets before analysis with EDX spectrum.

XRD analysis

The dried synthesized silver nanoparticles were analysed using an X-ray diffractometer (D8 Bruker, Germany) with Cu K_α radiation in the range of $30^o \leq 2\theta \leq 90°$ at 40 kV and 40 mA.

FTIR analysis

FTIR (PerkinElmer, US) spectra were obtained at room temperature in the spectral range between 480 and 4000 cm^{-1}. FTIR measurements were made to identify the possible biomolecules responsible for capping and efficient stabilization of the synthesized silver nanoparticles.

Study for the influence of different parameters

Influence of different temperatures (30, 40, 50, 60, 70, 80, 90 °C), pH values (3, 5, 7, 8, 11), bark extract amounts (2, 4, 6, 8, 10, 12, 14 mL), substrate concentrations (1, 3, 5, 7, 9, 11, 13 mM $AgNO_3$) and incubation periods (20, 40, 60, 80, 100, 120, 140 min) were investigated by varying the parameters one at a time. A sample of 1 mL was withdrawn at different time intervals and the absorbance was measured at 427 nm.

Measuring concentration of AgNPs using inductively coupled plasma optical emission spectrophotometer (ICP-OES)

The original concentration (80 mg/L) of the *Afzelia quanzensis* bark extract mediated AgNPs was measured using ICP-OES. Then, by diluting this solution, samples of different concentrations (10, 25, 50 mg/L) were used to investigate the concentration dependence of the antibacterial effect of Ag nanoparticles.

Evaluation of antibacterial activity of synthesized silver nanoparticles

The synthesized silver nanoparticles were tested for their antibacterial activity by using the disk diffusion method. The cultures of *Staphylococcus aureus* (ATCC-25923) and *Escherichia coli* (ATCC-39403) were obtained from American Type Culture Collection Center, USA. *S. aureus* and *E. coli* were grown on Mueller–Hinton agar medium. The disk diffusion was performed by placing different types of disks including bark extract (50 µL), synthesized silver nanoparticles (50 µL/10, 25, 50 mg/L), standard antibiotic (erythromycin 50 µL) and synthesized silver nanoparticles with standard antibiotic on the surface of the agar in plates and incubated for 24 h at 37 °C. The zones of inhibition were measured by the Hi-Media scale.

Results and discussion

Visual analysis

Afzelia quanzensis bark extract when incubated with $AgNO_3$ solution under dark conditions changed its colour from colourless to light reddish and finally to reddish brown. The colour of the filtrate changed to intense brown after 120 min of incubation (Fig. 2b, c). The control

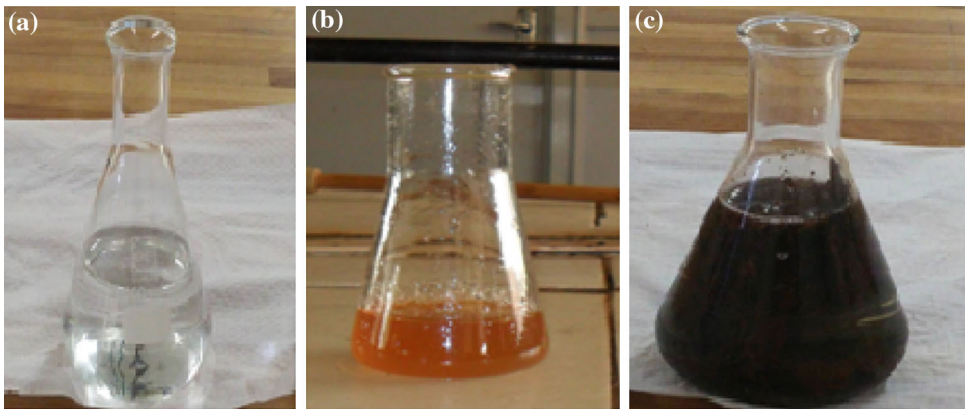

Fig. 2 Optical photograph of 1 mM $AgNO_3$ solution (**a**) filtrate with silver ions at the beginning of reaction (**b**) and after 120 min of reaction (**c**)

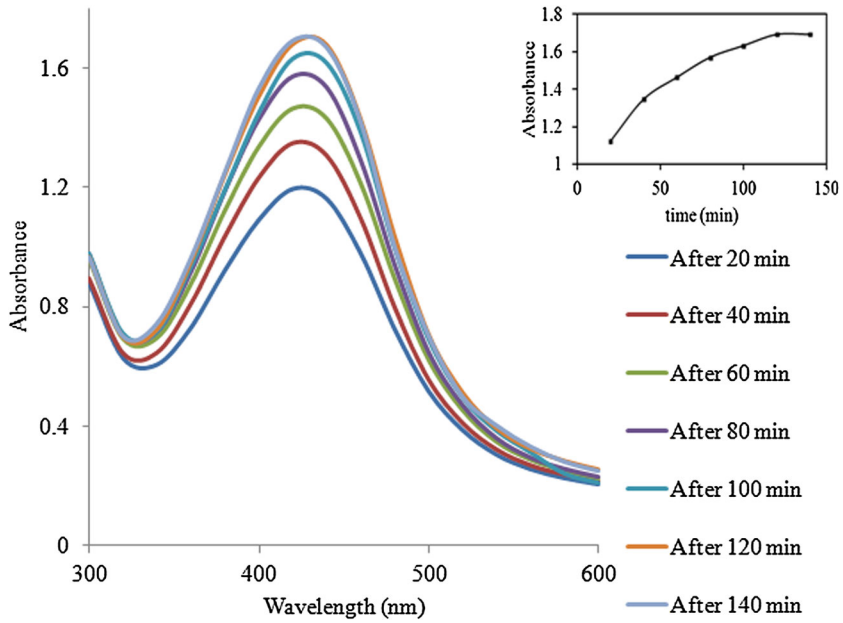

Fig. 3 The UV–visible absorption spectra of synthesized AgNPs. The *inset* shows the change in SPR as a function of time

$AgNO_3$ solution (without *Afzelia quanzensis* bark extract) showed no change in colour (Fig. 2a). The possible chemical reactions involved in the preparation of the AgNPs can be represented as:

$$Ag^{+}_{(aq)} + Afzelia\ quanzensis \xrightarrow[[\text{Stirring for 120 min at 70° C}]]{\text{Stirring at room temperature}} [Ag(Afzelia\ quanzensis)]^{+} \quad (1)$$

$$[Ag\ (Afzelia\ quanzensis)]^{+} + \text{R-CHO} \rightarrow [Ag\ (Afzelia\ quanzensis)] + \text{R-COOH} \quad (2)$$

UV–Vis spectra analysis

The development of metal silver nanoparticles in aqueous solution was described by UV–Vis spectroscopy. The absorption spectra of AgNPs formed at different durations are shown in (Fig. 3).

From Fig. 3, it can be observed that the plasmon band was symmetric, indicating that the solution does not have much aggregated particles [27]. The evolution of an absorption spectra for the AgNPs shows an increasingly sharp absorbance at 427 nm with increase in time, which steadily increased in intensity as a function of reaction time without showing any shift of the maximum wavelength [2]. This phenomenon may be linked to polarization of the free conduction electrons with respect to the much heavier ionic core of AgNPs, resulting in electron dipolar oscillation after exposure of AgNPs to light [12]. For quality assurance and comparison, $AgNO_3$ solution in deionized water showed no absorption peak at the same wavelength range (data not shown). In the present bark extract/Ag investigation, the reaction mixtures showed a single SPR band revealing the spherical shape of AgNPs which is in good agreement to the Mie's theory [28]. Consequently, this

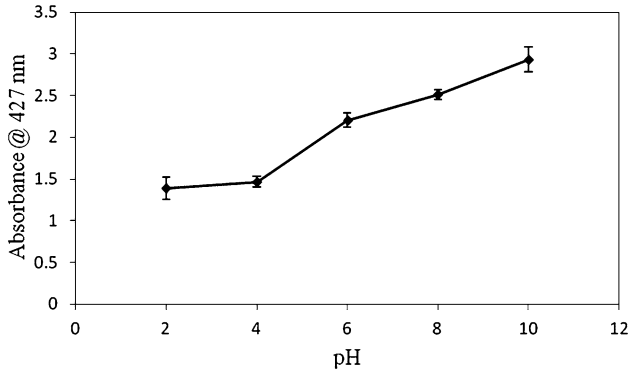

Fig. 4 Effect of different pH on nanoparticle production (*error bar* ±SD and $n = 3$)

validates the application of *Afzelia quanzensis* bark extract as a precursor for AgNPs synthesis.

Study for the influence of different parameters

The biosynthesis of AgNPs is affected by a variety of factors (substrate concentration, electron donor, incubation time, pH, temperature, buffer strength, etc.) which control the shape and size as well as achieving the monodispersity in solution phase. In this study, the effects of pH, $AgNO_3$ concentrations, different quantities of bark extract, and different temperatures were investigated.

Effect of pH

The size and morphology of nanoparticles are mainly affected by the pH of solution [29–31]. As shown by UV–Vis spectroscopy (Fig. 4), when the pH of the reaction mixture was increased, an increase in absorbance was observed. This might be due to the increase in production of colloidal silver nanoparticles and reduction rate. Visual observation showed the amount of nanoparticles to be pH value dependent. The reaction mixture colouring accelerated when the pH was increased. At acidic pH, large-sized silver nanoparticles were observed, whilst at higher pH highly dispersed, small-sized nanoparticles were formed. The results are in agreement with those reported in literature [32–34]. Control experiments ($AgNO_3$ solution incubated at different alkaline pH 8, 9, 10) showed no synthesis of nanoparticles.

Effect of $AgNO_3$ concentration

The concentration of $AgNO_3$ which might be converted to a final product is one of the important measures required to make the reaction more economical and efficient [31]. The effect of $AgNO_3$ concentration on synthesis of AgNPs is shown in Fig. 5.

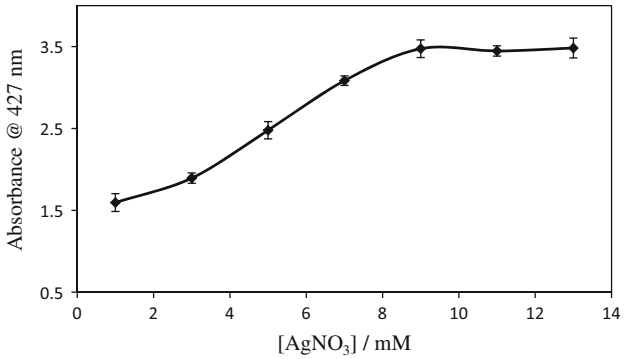

Fig. 5 Effect of $AgNO_3$ concentration (*error bar* ±SD and $n = 3$)

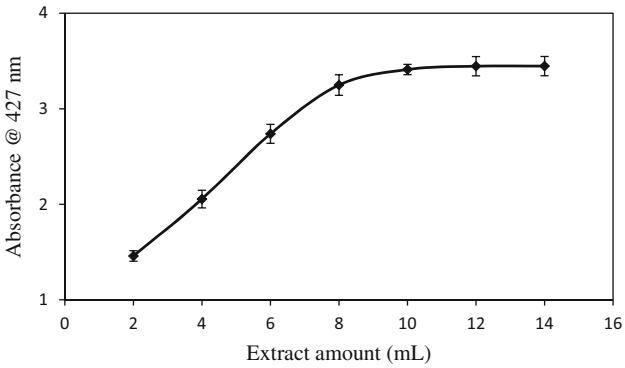

Fig. 6 Effect of different quantities of *Afzelia quanzensis* bark extract (*error bar* ±SD and $n = 3$)

There was an increase in synthesis of AgNPs with respect to Ag^+ ion concentration in the range 1–9 mM. However, the absorbance was found to decrease at concentrations greater than 9 mM. Comparable results were obtained for the synthesis AgNPs using *Pinus eldarica* bark extract [31]. Consequently, 9 mM was used for further studies.

Effect of different quantities of Afzelia quanzensis bark extract

The production of AgNPs was monitored as a function of different amounts of *Afzelia quanzensis* bark extract amount. Figure 6 shows the effect of extract amount on AgNPs production. The increase in the extract amount from 2 to 10 mL caused a considerable increase in peak absorbance in UV–Vis spectrum. The increase in the amount of soluble phytochemical reducing agents in the extract would mean more Ag^+ ion reduction, and subsequently more nanoparticle production. Furthermore, a decrease in amount of Ag nanoparticles was observed due to an increase in extract amount above 10 mL.

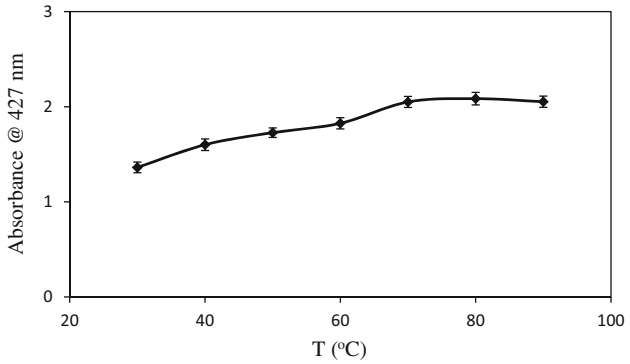

Fig. 7 Effect of reaction temperature (*error bar* ±SD; and $n = 3$)

Effect of temperature

The role of temperature on the reaction rate from 30 to 70 °C was investigated. An increase in absorbance was noted as the temperature increased (Fig. 7). The enhanced rate of synthesis of AgNPs might be due to the reaction temperature increasing the kinetic energy of the reacting molecules thus more Ag^{+} ions were in collision with the reducing molecules of the extract. The maximal synthesis of AgNPs was achieved at 70 °C.

Characterization

Electron microscopic study

The SEM images of the $AgNO_3$ (Fig. 8a) and synthesized silver nanoparticles (Fig. 8b) were clearly noticeable. The size of the silver nitrate particles used as control in this study was greater than 1 000 nm size (Fig. 8a); whereas, the synthesized silver nanoparticles measured 10–80 nm in size (Fig. 8b). Similar to our study, the same pattern of silver nanoparticles were also reported [24]. The EDAX spectroscopy results confirmed the significant presence of 61.66 % silver, 30.47 % carbon and oxygen 7.87 % (Fig. 9). Metallic silver nanocrystals generally show a typical optical absorption peak approximately at 3 keV due to surface plasmon resonance [35]. The weak signals at 0.25 and 0.50 keV were are for carbon and oxygen, respectively, which might arise from the functional compounds present in the aqueous extract.

XRD: purity and crystalline nature of AgNPs

The phase of the vacuum dried nanoparticles was investigated by XRD and corresponding patterns are shown in Fig. 10. However, silver nanoparticles have shown clear peaks of cubic phases (JCPDS No. 03-0921) at 38.1 (111), 42.9 (200), 65.5 (220) and 77.9 (311). XRD pattern thus

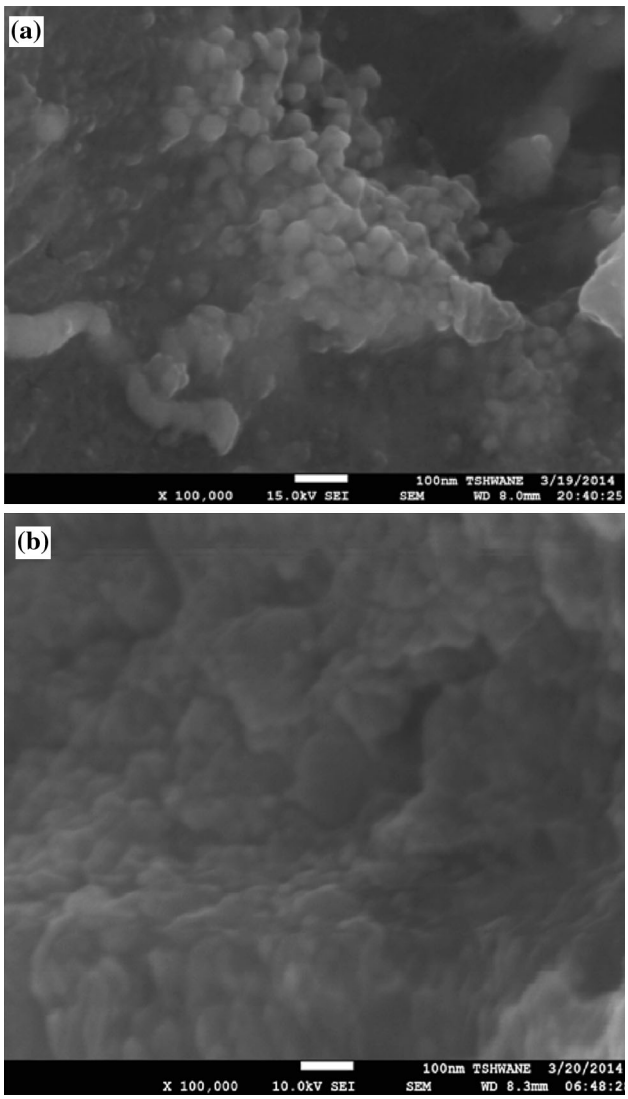

Fig. 8 Scanning electron microscopic observation of **a** silver nitrate and **b** synthesized

clearly illustrates that the silver nanoparticles formed in this present synthesis are crystalline in nature. There were no other corresponding peaks observed from the XRD pattern which showed that the formed AgNPs have a high purity. Previous studies have also reported the crystalline nature of biosynthesized AgNPs using different plant extracts [3, 9, 22, 23, 36]. The average crystalline size of silver nanoparticles synthesized using *Afzelia quanzensis* bark extract can be calculated using the Scherrer equation [25]:

$$D = \frac{K\lambda}{\beta Cos\theta}, \tag{3}$$

where D is the crystallite size of AgNPs, λ is the wavelength of the X-ray source (0.1541 nm), β is the full width at half maximum of the diffraction peak, K is the Scherrer

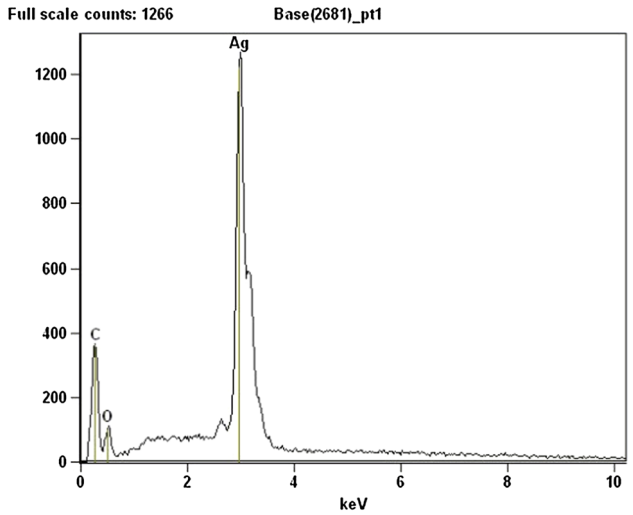

Fig. 9 The EDX spectrum for AgNPs

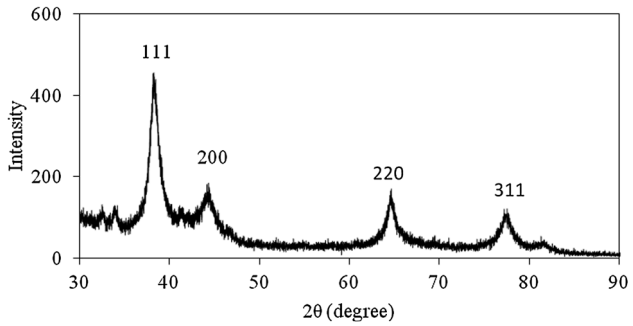

Fig. 10 XRD spectra of AgNPs

constant with a value from 0.9 to 1, and θ is the Bragg angle. The average crystalline size was 19.8 nm. The obtained average crystalline size coupled with the presence of structural peaks in XRD patterns clearly illustrated that the AgNPs synthesized were nanocrystalline in nature.

FTIR analysis

The FTIR spectra of *Afzelia quanzensis* extract and synthesized AgNPs were examined (Fig. 11). The strong band at 3455 cm^{-1} on the *Afzelia quanzensis* extract is characteristic of N–H and O–H stretching vibrations [35]. The characteristic absorption band at 2933 cm^{-1} is due to alkyl chains. The FTIR spectra also show bands at 1637 and 1445 cm^{-1} identified as amide I and amide II which arise due to carbonyl (C=O) and amine (–NH) stretching vibrations in the amide linkages of the proteins, respectively. The peaks at 1264 and 1060 cm^{-1} may be due to a carboxylate group (COO^{-}) and phosphate group, respectively. After reduction of $AgNO_3$, the band characteristic of N–H and O–H stretching vibrations shifted to 3424 cm^{-1}

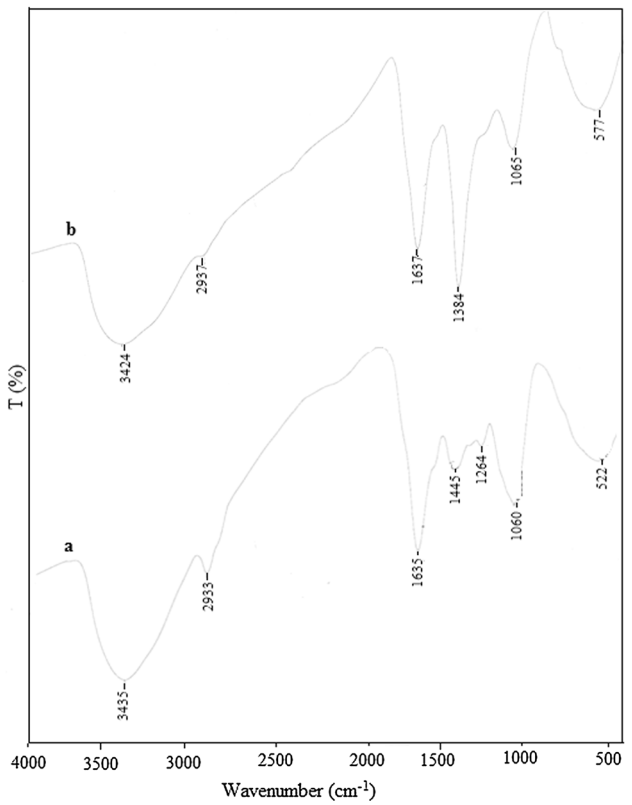

Fig. 11 FTIR spectra of *Afzelia quanzensis* extract (**a**) and synthesized AgNPs (**b**)

and alkyl group decreased in intensity, and shifted to 2937 cm^{-1}. The disappearance of the peaks at 1445 and 1264 cm^{-1} and formation of new intense peak at 1384 cm^{-1}, signify the involvement of the secondary amines in the reduction process. The shift of the band from 1635 to 1637 cm^{-1} is attributed to the binding of (NH) CO group with nanoparticles. It can be concluded from the FTIR study that the carboxyl (–C=O) and amine (N–H) groups in *Afzelia quanzensis* bark extract were mainly involved in reduction of Ag^{+} ions to Ag^{0} nanoparticles.

Stability studies

A vital aspect in colloid chemistry is how nano-scale particles are stabilized in their reaction media as smaller particles are prone to agglomeration. The stability of the AgNPs in solution was checked using UV–Vis spectroscopy by observing changes in the SPR band peak [37]. Figure 12 shows UV–Vis spectra periodically obtained over 60 days. The AgNPs produced from bark extract were observed to be very stable in solution when monitored periodically over a period of 40 days; with no evidence of flocculation or change in SPR, measured at 427 nm. However, after 50 days the surface plasmon resonance absorption band decreased and can be attributed to

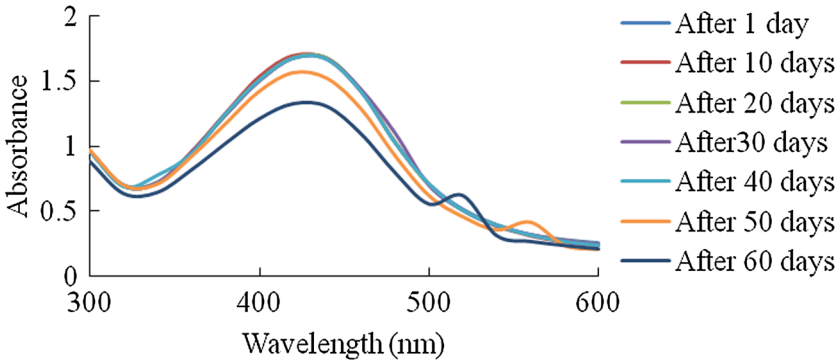

Fig. 12 Stability studies

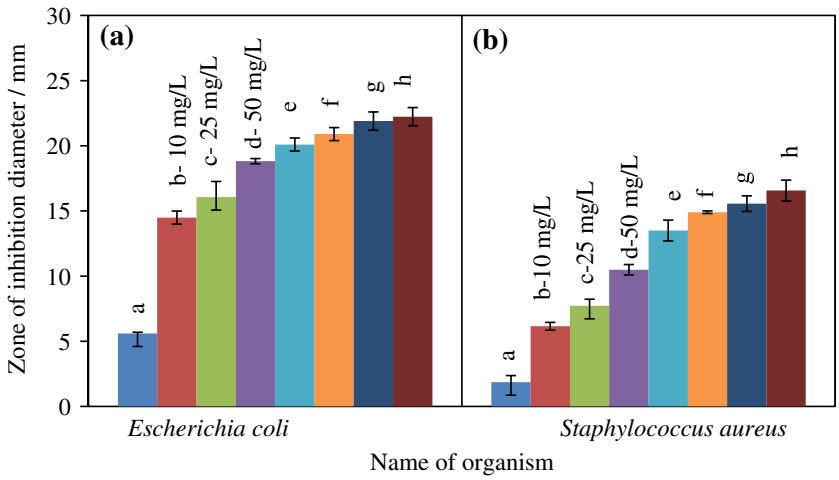

Fig. 13 Graphical representation of inhibition zones by plant extract (*a*), 10 mg/L synthesized AgNPs (*b*), 25 mg/L synthesized AgNPs (*c*), 50 mg/L synthesized AgNPs (*d*), erythromycin (*e*), erythromycin plus 10 mg/L synthesized AgNPs (*f*), erythromycin plus 25 mg/L synthesized AgNPs (*g*), erythromycin plus 50 mg/L synthesized AgNPs (*h*), for **a** *Escherichia coli*, **b** *Staphylococcus aureus* (*error bar* ±SD and $n = 3$)

destabilization of AgNPs in solution due to aggregation. Between 50 and 60 days secondary peaks appear at longer wavelength which is a sign of destabilization.

Evaluation of antibacterial activity of synthesized silver nanoparticles

The antimicrobial activity of bark extract (a), synthesized AgNPs of different concentrations (b–d), the antibiotic (erythromycin) (e) and antibiotic plus different concentrations of synthesized AgNPs (f–h) were evaluated by diffusion method. The bacterial cultures used were Gram-positive bacteria, i.e. *Staphylococcus aureus* and Gram-negative bacteria, i.e. *Escherichia coli*. The increase in zone of inhibition of silver nanoparticles at different concentrations (10, 25, 50 mg/L) compared with antibiotic for both bacterial cultures (Fig. 13a, b) demonstrated the lesser antibacterial potential of silver nanoparticles with that of antibiotics. The zone of inhibition also increased with AgNPs concentration in both cultures. The bark extract exhibits the highest activity against *E. coli* than *S. aureus*. The obtained results support, at least in part, the use of this plant as traditional medicine against Gram-negative bacteria due to the presence of phytochemicals. Furthermore, the phytofabricated silver nanoparticles were found to be more effective against *Escherichia coli* as compared to that of *Staphylococcus aureus*. From Fig. 13a, b, it can be confirmed that combining the antibiotics with AgNPs resulted in a greater bactericidal effect on test pathogens than either of the antibacterial agents used alone. Inhibition of *Escherichia coli* might have been facilitated by silver's high affinity for phosphorus and sulphur which are part of the cell membranes of Gram-negative bacteria [38]. The sulphur and phosphorus reacts with AgNPs causing dysfunction of enzymes on bacteria cell wall and also it disturbs DNA's moieties process thereby denying replication [39]. On the other hand, the cell wall of Gram-positive bacteria is much more rigid due to the presence of a thick peptidoglycan layer, which is superficial to the cell membrane hence a difference in activity observed.

Conclusion

The silver nanoparticles were green synthesized using bark extract of *Afzelia quanzensis*. The method represents an example of clean, nontoxic and eco-friendly method for obtaining silver nanoparticles. Colour changes occur due to

surface plasmon resonance during the reaction with *Afzelia quanzensis* bark extract resulting in the formation of silver nanoparticles, which was confirmed by XRD, FTIR, UV–Vis spectroscopy, and EDAX. The silver nanoparticles were found to be stable in water for 40 days. The zone of inhibition test showed that the synthesized nanoparticles have some antibacterial activity. Further studies will be conducted to isolate and quantify the different phytochemical components and to study their pharmacological properties after synthesizing the silver nanoparticles from the specific phytochemicals.

Compliance with ethical standards

Conflict of interest The authors have no conflict of interest.

References

1. Kathiresan K, Manivannan S, Nabeel MA, Dhivya B (2009) Studies on silver nanoparticles synthesized by a marine fungus, *Penicillium fellutanum* isolated from coastal mangrove sediment. Colloids Surf 71:133–137
2. Sridhara V, Pratima K, Krishnamurthy G, Sreekanth B (2013) Vegetable assisted synthesis of silver nanoparticles and its antibacterial activity against two human pathogens. Asian J Pharm Clin Res 6:53–57
3. Awwad AM, Salem NM, Abdeen AO (2013) Green synthesis of silver nanoparticles using carob leaf extract and its antibacterial activity. Intern J Indust Chem 4:29–35
4. Peterson MSM, Bouwman J, Chen Deutsch AM (2007) Inorganic metallodielectric materials fabricated using two single-step methods based on the Tollen's process. J Colloid Interface Sci 306:41–49
5. Shao K, Yao J (2006) Preparation of silver nanoparticles via a non-template method. Mater Lett 60:3826–3829
6. Tsuji T, Iryo K, Watanabe N, Tsuji M (2002) Preparation of silver nanoparticles by laser ablation in solution: influence of laser wavelength on particle size. Appl Surf Sci 202:80–85
7. Nagaraz B, Krishnamurthy NB, Liny P, Divya TK, Dinesh R (2011) Biosynthesis of gold nanoparticles of *Ixora coccinea* flower extract and their antimicrobial activities. Int J Pharma Bio Sci 2:557–565
8. Bar H, Bhui DK, Sahoo GP Sarkar P, De SP, Misra A (2009) Green synthesis of silver nanoparticles using latex of *Jatropha curcas*. Colloids Surf 339:134–139
9. Bar H, Bhui DK, Sahoo GP, Sarkar P, Pyne S, Misra A (2009) Green synthesis of silver nanoparticles using seed extract of *Jatropha curcas*. Colloids Surf A 348:212–216
10. Das VL, Thomas R, Varghese RT, Soniya EV, Mathew J, Radhakrishnan EK (2014) Extracellular synthesis of silver nanoparticles by the *Bacillus* strain CS 11 isolated from industrialized area3. Biotech 4(2):121–126
11. Ghorbani HR (2013) Biosynthesis of silver nanoparticles using *Salmonella typhirium*. J Nanostruct Chem 3(29):1–4
12. Swarup R, Kumar DT (2014) Biosynthesis of silver nanoparticles by *Aspergillus foetidus*: optimization of physicochemical parameters. Nanosci Nanotechnol Lett 6(3):181
13. Prasad K, Anal KJ, Kulkarni AR (2007) Lactobacillus assisted synthesis of titanium nanoparticles. Nanoscale Res Lett 2:248–250
14. Jha AK, Kamalesh P, Prasad K (2009) A green low-cost biosynthesis of Sb_2O_3 nanoparticles. Biochem Eng J 43:303–306
15. Hebbalalu D, Lalley J, Nadagouda MN, Varma RS (2013) Greener techniques for the synthesis of silver nanoparticles using plant extracts, enzymes, bacteria, biodegradable polymers, and microwaves. ACS Sustain Chem Eng 1(7):703–712
16. Prathap M, Alagesan A, Ranjitha Kumari BD (2014) Anti-bacterial activities of silver nanoparticles synthesized from plant leaf extract of *Abutilon indicum* (L.) Sweet. J Nanostruct Chem 4:106
17. Lee SH, Salunke BK, Kim BS (2014) Sucrose density gradient centrifugation separation of gold and silver nanoparticles synthesized using *Magnolia kobus* plant leaf extracts. Biotechnol Bioprocess Eng 19:169–174
18. Murugan K, Senthilkumar B, Senbagam D, Al-Sohaibani S (2014) Biosynthesis of silver nanoparticles using *Acacia leucophloea* extract and their antibacterial activity. Int J Nanomed 9:2431–2438
19. Maria BS, Devadiga A, Kodialbail VS, Saidutta MB (2015) Synthesis of silver nanoparticles using medicinal *Zizyphus xylopyrus* bark extract. Appl Nanosci 5:755–762
20. Chandran SP, Chaudhary M, Pasricha R, Ahmad A, Sastry M (2006) Synthesis of gold nanotriangles and silver nanoparticles using *aloevera* plant extract. Biotechnol Progress 22:577–583
21. Sharma NC, Sahi SV, Nath S, Parsons JG, Gardea-Torresdey JL, Pal T (2007) Synthesis of plant-mediated gold nanoparticles and catalytic role of biomatrix embedded nanomaterials. Environ Sci Technol 41:5137–5142
22. Sathishkumar M, Sneha K, Won SW, Cho CW, Kim S, Yun YS (2009) *Cinnamon zeylanicum* bark extract and powder mediated green synthesis of nano-crystalline silver particles and its bactericidal activity. Colloids Surf B 73:332–338
23. Sathishkumar M, Sneha K, Yun YS (2010) Immobilization of silver nanoparticles synthesized using curcuma longa tuber powder and extract on cotton cloth for bactericidal activity. Bioresour Technol 101:7958–7965
24. Bhati-Kushwaha H, Malik CP (2014) Biosynthesis of silver nanoparticles using fresh extracts of *Tridax procumbens* Linn. Indian J Exp Biol 52:359–368
25. Ahmad N, Sharma S, Alam MK, Singh VN, Shamsi SF, Mehta BR, Fatma A (2010) Rapid synthesis of silver nanoparticles using dried medicinal plant of basil. Colloids Surf B 81:81–86
26. Biegel HM (1977) Check-list of ornamental plants used in Rhodesian parks and gardens. Rhod Agric J Res Rep 3:19–20
27. Link S, El-Sayed MA (1999) Spectral properties and relaxation dynamics of surface plasmon electronic oscillations in gold and silver nanodots and nanorods. J Phys Chem B 103:8410–8426
28. Ghadimi A, Saidur R, Metselaar HSC (2011) A review of nanofluid stability properties and characterization in stationary conditions. Int J Heat Mass Transf 54:4051–4068
29. Konishi Y, Tsukiyama TTT, Saitoh N, Nomura T, Nagamine S (2007) Microbial deposition of gold nanoparticles by the metal-reducing bacterium *Shewanella algae*. Electrochim Acta 53:186–192
30. Sanghi R, Verma P (2009) Biomimetic synthesis and characterisation of protein capped silver nanoparticles. Bioresour Technol 100:501–504
31. Iravani S, Zolfaghari B (2013) Green synthesis of silver nanoparticles using *pinus bark* extract. Biomed Res Int 2013:1–5

32. Gardea-Torresdey JL, Tiemann KJ, Gamez G, Dokken K, Tehuacanero S, Jośe-Yacaḿan M (1999) Gold nanoparticles obtained by bio-precipitation from gold (III) solutions. J Nanopart Res 1:397–404
33. Birla SS, Gaikwad SC, Gade AK, Rai MK (2013) Rapid synthesis of silver nanoparticles from fusarium oxysporum by optimizing physicocultural conditions. Sci World J 2013:1–12. doi:10.1155/2013/796018
34. Armendariz V, Herrera I, Peralta-Videa JR (2004) Size controlled gold nanoparticle formation by *Avena sativa* biomass: use of plants in nanobiotechnology. J Nanopart Res 6:377–382
35. Das SK, Khan MMR, Guha AK, Das AR, Mandal AB (2012) Silver-nano biohybride material: synthesis, characterization and application in water purification. Bioresour Technol 124:495–499
36. Krishnaraj C, Jagan EG, Rajasekar S, Selvakumar P, Kalaichelvan PT, Mohan N (2010) Synthesis of silver nanoparticles using *Acalypha indica* leaf extracts and its antibacterial activity against water borne pathogens. Colloids Surf B 76:50–56
37. Lee DK, Tho NTM, Minhan TN, Tri MD, Sreekanth TVM, Lee JS, Nagajyothi PC (2013) Green synthesis of silver nanoparticles using *Nelumbo nucifera* seed extract and its antimicrobial activity. Acta Chim Slov 60:673–678
38. Hari N, Thomas TK, Nair AJ (2014) Comparative study on the synergistic action of differentially synthesized silver nanoparticles with β-Cephem antibiotics and chloramphenicol. J Nanosci 2014:1–8
39. Shetty P, Supraja N, Garud M, Prasad TNVKV (2014) Synthesis, characterization and antimicrobial activity of *Alstonia scholaris* bark-extract-mediated silver nanoparticles. J Nanostruct Chem 4(4):161–170